International Journal of Pharmaceutics 388 (2010) 280–286

Contents lists available at ScienceDirect

International Journal of Pharmaceutics

journal homepage: www.elsevier.com/locate/ijpharm

Pharmaceutical nanotechnology

Layered bionanocomposites as carrier for procainamide

Bhavesh D. Kevadiya, Ghanshyam V. Joshi, Hari C. Bajaj*

Discipline of Inorganic Materials and Catalysis, Central Salt and Marine Chemicals Research Institute, Council of Scientific and Industrial Research (CSIR), Gijubhai Badheka Marg, Bhavnagar 364 002, Gujarat, India

ARTICLE INFO

Article history:
Received 28 August 2009
Received in revised form
30 December 2009
Accepted 6 January 2010
Available online 13 January 2010

Keywords:
Procainamide hydrochloride (PA)
Montmorillonite (MMT)
Control release
Nanocomposites

ABSTRACT

The study deals with the intercalation of procainamide hydrochloride (PA), an antiarrythmia drug in montmorillonite (MMT), as a new drug delivery device. Optimum intercalation of PA molecules within the interlayer space of MMT was achieved by means of different reaction conditions. Intercalation of PA in the MMT galleries was conformed by X-ray diffraction (XRD), Fourier transform infrared spectra (FT-IR), and thermal analysis (DSC). In order to retard the quantity of drug release in the gastric environment, the prepared PA–MMT composite was compounded with alginate (AL), and further coated with chitosan (CS). The surface morphology of the PA–MMT–AL and PA–MMT–AL–CS nanocomposites beads was analyzed by scanning electron microscope (SEM). The in vitro release experiments revealed that AL and CS were able to retard the drug release in gastric environments, and release the drug in the intestinal environments with a controlled manner. The release profiles of PA from composites were best fitted in Higuchi kinetic model, and Korsmeyer–Peppas model suggested diffusion controlled release mechanism.

1. Introduction

For controlled drug delivery systems, the optimal concentration of drug should be maintained without reaching a higher toxic level or dropping below the minimum effective level. Recently, the field of polymer layered silicate composites has attracted much attention for drug delivery applications (Pongjanyakul, 2009). The unique properties of the polymer layered silicate composites such as easy degradation, biocompatibility and tunable mechanical properties are essential for pharmaceutical applications (Pongjanyakul, 2009). Montmorillonite (MMT), smectite family clay is a promising layered silicate as delivery carrier for various drug molecules. Smectite clays have a layered structure and layer is constructed from tetrahedrally coordinated silica atoms fused into an edge-shared octahedral plane of aluminum. (Mohanambe and Vasudevan, 2005; Patel et al., 2006; Depan et al., 2009). Moreover, the positively charged edges on the layers of MMT could interact with anionic polymer like alginate (AL) to form unique polymer layered silicate materials having a large inter-planar spacing; and superior capability to intercalate drug molecules into the interlayer space of the (0 0 1) plane. Involvement of MMT to AL composites decreases the drug release rate due to an increase in the adsorption capacity for the incorporated compound by the matrix (Gerstl et al., 1998; Lin et al., 2002; Pongjanyakul, 2009).

Alginate (AL) is widely used as a drug delivery vehicle for control release of therapeutic agents (Shilpa et al., 2003). The capability of AL to form gel in the presence of multivalent ions has been exploited to prepare multi-particulate systems, incorporating numerous drugs, proteins, cells, or enzymes. AL is a linear, naturally occurring polysaccharide extracted from brown sea algae containing D-mannuronic (M) and L-guluronic (G) acids which are arranged in homopolymeric MM or GG blocks separated by blocks with an alternating sequence (Tonnesen and Karlsen, 2002). The distinctive properties of AL, e.g. hydrophilicity, biocompatibility, mucoadhesiveness, nontoxicity, and inexpensiveness makes it a potential drug delivery carrier. AL shrinks at low pH (gastric environment) and the encapsulated drugs cannot be released in the stomach, this phenomenon leads to site-specific delivery (Shilpa et al., 2003). The hydrogel of AL have attracted increasing attention due to their unique properties of pH-sensitivity as drug carrier (Shilpa et al., 2003). Due to increase in pH as the hydrogels pass down the intestinal tract, the degree of swelling increases which facilitate its rapid disintegration and drug releases at preferred sites (Tonnesen and Karlsen, 2002). The chitosan (CS), copolymer of D-glucosamine and N-acetyl glucosamine derived from chitin deacetylation process has a special feature of adhesion to the mucosal surface and transiently opening of tight junction between epithelial cells therefore quiet appropriate for drug carriers (Denkbas and Ottenbrite, 2006; Wang et al., 2008). Compared to other biopolymers, AL and CS offer additional advantage in terms of safety, biocompatibility and low cost.

Although several drugs have been extensively investigated using alginate, chitosan and synthetic peptide as carriers, but

* Corresponding author. Tel.: +91 278 2471793; fax: +91 278 2567562.
E-mail address: hcbajaj@csmcri.org (H.C. Bajaj).

0378-5173/$ – see front matter © 2010 Elsevier B.V. All rights reserved.
doi:10.1016/j.ijpharm.2010.01.002

the use of layered silicate along with AL and CS as carrier is inadequate. Lin et al. (2006) have modified the MMT gallery by trimethylammonium cation (HDTMA) and used it as DNA carrier. Poly(D,L-lactide-co-glycolide)/MMT nanoparticles for targeted breast cancer chemotherapy of paclitaxel have been reported (Dong and Feng, 2005; Sun et al., 2008). Various drug molecules such as BSA (Wang et al., 2008), timolol maleate, vitamin B_1 and vitamin B_6 (Joshi et al., 2009a,b,c; Kevadiya et al., 2009), carbofuran (Manuel Fernandez-Perez et al., 2000), ibuprofen (Zheng et al., 2007), donepezil (Park et al., 2008) have been studied to execute controlled drug delivery using smectite clays. Procainamide hydrochloride (PA, an antiarrythmia drug), has a short half-life in vivo and it must be dosed in every 3–4 h (Danielly et al., 1994; Sintov and Levy, 1997; Ellenbogen et al., 1998; Markland et al., 1999; Lee et al., 2005; An et al., 2009).

The present communication deals with the intercalation of PA molecules into the interlayer of MMT at different reaction environment such as time, temperature, pH, and initial concentration. In order to control the release of PA in the gastric environments, PA–MMT composites were compounded with natural polymers, AL and CS. The in vitro drug release studies were performed using buffer solutions of pH 1.2 and 7.4. Higuchi and Korsmeyer–Peppas kinetic models were applied to elucidate the drug release kinetics in a superior way.

2. Materials and methods

2.1. Materials

Alginic acid sodium salt (viscosity: 20.0–40.0 CP in 1% water, MW: 7334), procainamide hydrochloride (PA), chitosan (medium molecular weight) and cellulose acetate dialysis tube (MW: 07014) were purchased from Sigma–Aldrich, USA. Sodium chloride, fused calcium chloride, hydrochloric acid, potassium chloride, potassium dihydrogen orthophosphate and sodium hydroxide were procured from S.D. fine chemicals, India and were used as received. The montmorillonite (MMT) rich bentonite clay was collected from Akli mines, Barmer district, Rajasthan, India. Deionized water was obtained from Milli-Q Gradient A10 water purification system.

2.2. Preparation of PA–MMT composites

2.2.1. Purification of MMT

300 g of raw bentonite dispersed in 3 l of 0.1 M NaCl solution was stirred for 12 h. To obtain Na-MMT, the slurry was treated with NaCl for three times. Finally, the slurry was centrifuged and washed with Milli-Q water until free from chloride ion as tested by $AgNO_3$ solution (Bergaya et al., 2006). Na-MMT was purified by sedimentation technique as described earlier (Patel et al., 2007a). The cation exchange capacity of MMT (91 mequiv./100 g of MMT on dry basis, dried at 110 °C) was measured by the standard ammonium acetate method at pH 7 (Bergaya et al., 2006).

2.2.2. Intercalation kinetics

20 ml aqueous solution of PA (120 mg of PA) was mixed with 100 mg of MMT powder in 100 ml conical flask. The experiments were performed with continuous shaking (Julabo shaking water bath, SW23) at 40 °C, and different time intervals ranging from 1 to 24 h. The reaction mixtures were filtered and analyzed for PA by UV–visible spectrophotometer at λ_{max} = 278 nm. The amount of PA intercalated per gram of MMT was calculated by the difference of the PA concentration before and after the intercalation process.

2.2.3. Effect of temperature

100 mg of MMT was dispersed in 20 ml of deionized water containing 120 mg of PA. The suspensions were shaken for 5 h, and at 30, 40, 50, 60, 70, and 80 °C. The reaction mixtures were filtered, and the concentration of PA in the filtrate was determined spectrophotometrically.

2.2.4. Influence of pH environment

The relation between pH and the intercalation amount of PA in MMT was studied at optimized time (5 h), temperature (40 °C), and fixed concentration of PA (120 mg). 20 ml aqueous solution of PA and 100 mg of MMT powder were taken in a 100 ml flask, and was shaken. The pH was adjusted from 2 to 12 by HCl and NaOH solutions. The remaining concentrations of PA in the filtrates were measured by UV absorbance.

2.2.5. Equilibrium isotherms

To study the effect of PA concentration on the intercalation of PA into MMT, reactions were carried out at different initial concentration of PA at constant time, temperature, and pH. 20 ml aqueous solution of PA containing different amount of PA were treated with 100 mg of MMT powder for 5 h, at pH 4 and 40 °C in a 100 ml conical flask with continuous shaking. The reaction mixtures were filtered and absorption of PA in the filtrates was determined by UV–visible spectrophotometer. The entire intercalation studies were performed in triplicate and the average values were utilized in data analysis.

2.2.6. Characterization

Powder X-ray diffraction (PXRD) analysis were carried out with a Phillips powder diffractometer X'Pert MPD using PW3123/00 curved Ni-filtered Cu Kα (λ = 1.54056 Å) radiation with scanning of 0.3°/s in 2θ range of 2–10°. Fourier transform infrared spectra (FT-IR) were recorded on PerkinElmer, GX-FT-IR as KBr pellet over the wavelength range 4000–400 cm^{-1}. Differential scanning calorimetric (DSC) studies were carried out in the range of 30–400 °C at the rate 10 °C/min under nitrogen flow (10 ml/min) using Mettler-Toledo, DSC-822e, Switzerland. The morphology of composites beads was observed by scanning electron microscope (SEM), LEO-1430VP, UK. The UV–visible absorbance of procainamide hydrochloride solutions were measured on UV–visible spectrophotometer (Shimadzu, UV-2550, Japan) equipped with a quartz cell having a path length of 1 cm.

2.3. Preparation of PA–MMT–AL composites

The site-specific delivery of PA was attained by compounding the prepared PA–MMT composite with AL, and further coated with CS. The appropriate amount of AL (1.0 g) dissolved in deionized water (50 ml) and stirred for 6–8 h to obtain homogeneous solution. The required quantity of calcium chloride dihydrate was dissolved in deionized water to prepare 100 mmol solutions. PA–MMT–AL nanocomposite beads were prepared by the means of gelation technique (Shilpa et al., 2003; Pasparakis and Bouropoulos, 2006; Dai et al., 2008). Appropriate amount of PA loaded MMT (0.7 g) was added to the AL solution, and stirred for 5 h to obtain homogeneous suspension. The resulting solution was then slowly added to the 200 ml calcium chloride solution by dripping it from the tip of a 20-guage hypodermic needle (falling distance 2 cm, pumping rate 2.5 ml/min) attached to a peristaltic pump (Master flex L/S 7518-00, Cole-Parmer, USA). In this approach the spherical shape of the drop was retained by the gelled suspension. The beads were allowed to cure in the calcium chloride solution for 20 min, and then separated by filtration. The prepared beads were washed thrice with deionized water, and dried at room temperature. The filtrate was used to calculate the encapsulation efficiency of the beads. The mean diameter of the dry beads was determined by measuring 50 beads with the help of micrometer screw (Mitutoyo, Japan), and mean value was used for data analysis. The PA–MMT composite: alginate

Table 1
Different parameters of PA–MMT composites formulations.

Parameters	PA–MMT–AL
Encapsulation efficiency (%)	91.04
Drug loading (%)	8.53
Bead diameter (mm)	0.61

ratio (1:1.4%, w/w) was optimized to obtain stable beads, having minimum amount of alginate and controlled release profiles.

2.4. Preparation of CS coated PA–MMT–AL composites

For coating of PA–MMT–AL nanocomposite beads with CS, 0.5% (w/v) CS solution was prepared by dissolving the desired quantity of CS into deionized water, and the pH was adjusted to 1.2 using HCl. The PA–MMT–AL nanocomposite beads, prepared above were added to 50 ml of CS solution, kept for 20 min under gentle stirring and finally the beads were collected by filtration, and dried at room temperature.

2.5. Encapsulation efficiency

The amount of PA captured into the PA–MMT–AL nanocomposites beads were calculated by measuring the absorbance of the gelling medium at 278 nm. The encapsulation efficiency (EE%) was calculated as:

$$\mathrm{EE}(\%) = \left\{ \frac{(W_i - W_d)}{W_i} \right\} \times 100 \quad (1)$$

where W_i initial weight of PA dissolved in the AL solution and W_d weight of PA measured in the gelling media after the preparation of the drug-loaded beads.

The drug content (DC%) was calculated as

$$\mathrm{DC}(\%) = \left\{ \frac{M_i}{M_d} \right\} \times 100 \quad (2)$$

where M_i the weight of PA in coated composites and M_d the weight of coated composites (Table 1).

2.6. In vitro release study

In vitro release behavior of PA was carried out with the help of USP eight stage dissolution rate test apparatus (VEEGO, Mumbai, India) using dialysis bag technique (Joshi et al., 2009a,b; Kevadiya et al., 2009). The PA release experiments were carried out at pH 1.2 (1000 ml of 0.2 M HCl and 588 ml of 0.2 M KCl) and at pH 7.4 (1000 ml of 0.1 M KH_2PO_4 and 782 ml of 0.1 M NaOH). The dialysis bags were equilibrated with the release medium for few hours prior to release studies. The weighed quantities of beads (containing 20 mg of PA) were placed in dialysis bag containing 5 ml of the release medium. The dialysis bags were placed in stainless steel baskets and were immersed in container containing 500 ml of release medium. The temperature was maintained to $37 \pm 0.5\,^{\circ}C$ and rotation frequency of basket was kept at 100 rpm. 1 ml of aliquots was withdrawn at regular time interval and the same volume was replaced with a fresh release medium. Samples were further diluted and analyzed for PA content by UV–visible spectrophotometer. These studies were performed in triplicate for each sample and the average values were used in data analysis.

2.7. Drug release kinetics

In order to understand the drug release mechanisms, the results obtained were fitted in two kinetic models; Higuchi and Korsmeyer–Peppas. The Higuchi model describes the release of drugs as a square root of time based on fickian diffusion (Eq. (3)).

$$Q = k_H t^{1/2} \quad (3)$$

k_H is the constant reflecting the design variables of the system.

Korsmeyer et al. (1983) derived a relationship for drug release kinetics (Eq. (4)). To find out the mechanism of drug release during the first 10 h, drug release data was fitted by the Korsmeyer–Peppas model.

$$\frac{M_t}{M_\infty} = Kt^n \quad (4)$$

where M_t/M_∞ is the fraction of drug released at time t, K is the rate constant and n is the diffusion exponent. According to this model, the value of n identifies the release mechanism of drug. Values of n between 0.5 and 1.0 indicate anomalous transport kinetics, n approximately 0.5 indicates the pure diffusion controlled mechanism (fickian diffusion). The smaller values $n < 0.5$ may be due to drug diffusion partially through a swollen matrix and water filled pores in the formulations (Pasparakis and Bouropoulos, 2006; Joshi et al., 2009b).

3. Results and discussion

3.1. Preparation of PA–MMT composites

3.1.1. Intercalation kinetics

Ion exchange reaction between the interlayer Na^+ ions of MMT and cationic PA molecules in the aqueous media is responsible for the intercalation process. About 24.4% of PA was intercalated into MMT within 3 h of interaction time, which remained constant up to 24 h. To avoid the partial intercalation of PA molecules in MMT, the interaction time was set to 5 h in the subsequent experiments.

3.1.2. Influence of pH environment

The pH of the drug solution has always played a crucial role for the intercalation between cationic molecules and MMT layers (Lin et al., 2002; Joshi et al., 2009a,b,c). The intercalation of PA in MMT remains constant in the pH range 4–9 (Fig. 1), and it decreases above pH 9 and below pH 4.The PA exists as mono charged cations below pH ≤ 7.5 (pK_a of PA is ~9.45). Intercalation at pH 12 is only about 6.3%, due to largely uncharged PA species and below pH 4, there was a decrease in adsorption of PA in the clay lattice due to the competition between the cationic drug and H^+ ions present as exchangeable ion in MMT (Joshi et al., 2009a).

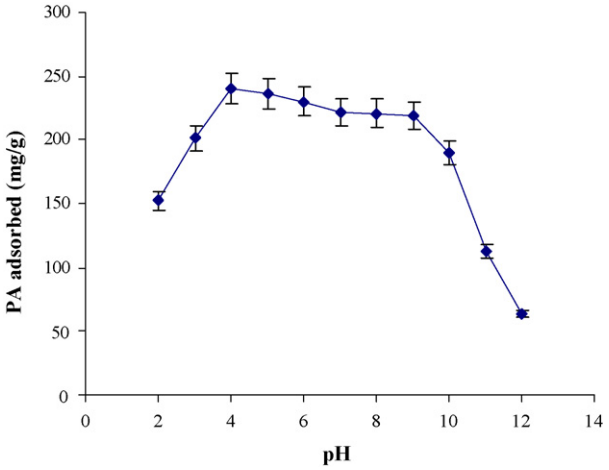

Fig. 1. Influence of pH on PA intercalation (MMT = 100 mg, PA = 120 mg/20 ml, temperature = 40 °C, and time = 5 h).

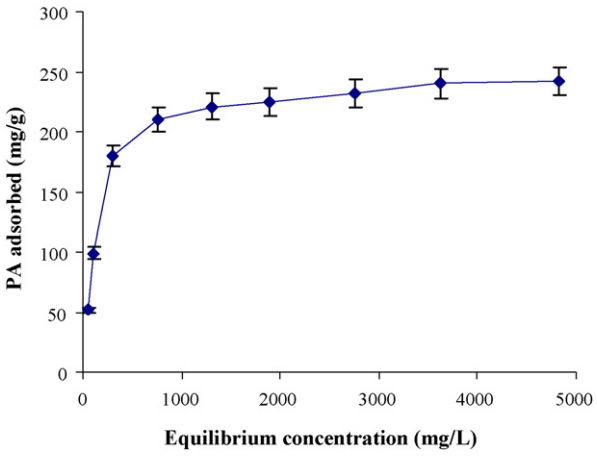

Fig. 2. Relation between adsorption of PA and initial concentration (MMT = 100 mg, pH = 4, temperature = 40 °C, and time = 5 h).

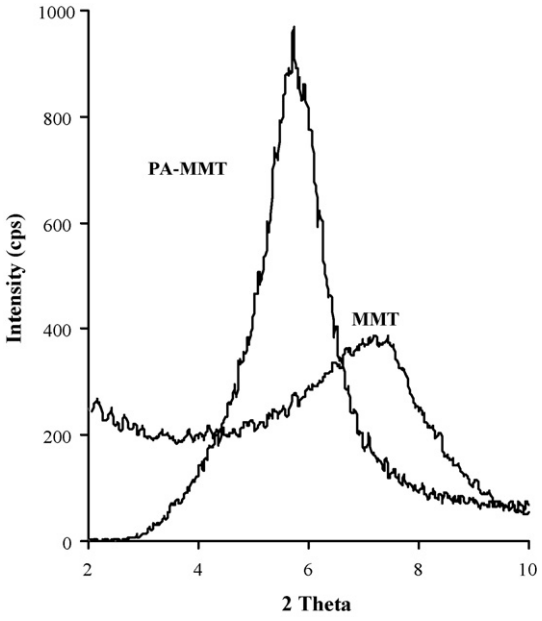

Fig. 3. XRD patterns of MMT and PA–MMT composites.

3.1.3. Effect of temperature

The amount of PA adsorbed on MMT at different temperatures is as follows: 224.7 ± 2.8, 244 ± 2.2, 229.7 ± 2.4, 232 ± 2.4, 233.7 ± 4.2 and 236 ± 7.1 mg/g at 30, 40, 50, 60, 70 and 80 °C, respectively. There was no considerable change in the adsorption with temperature.

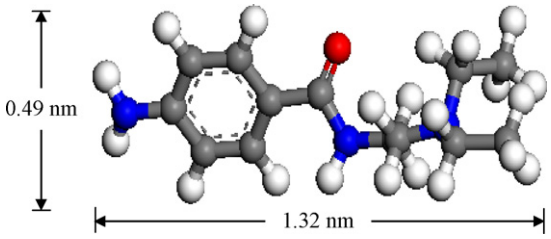

Fig. 4. Three-dimensional molecular structure of PA.

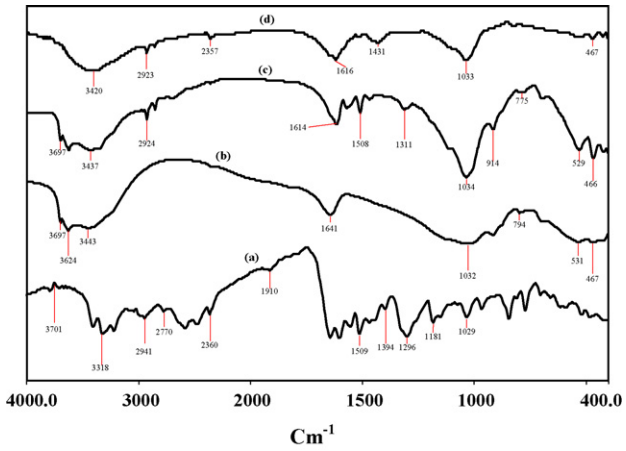

Fig. 5. FT-IR spectra of (a) PA, (b) MMT, (c) PA–MMT and (d) PA–MMT–AL.

3.1.4. Equilibrium isotherms

Intercalation of PA into MMT layers is highly concentration dependent. As the initial concentration of PA increases, the amount of intercalation increased due to concentration gradient (Fig. 2). However, it reached equilibrium after intercalation of 244 mg of PA/g of MMT.

3.2. Characterization

3.2.1. XRD and FT-IR analysis

The XRD pattern of pure MMT and PA–MMT composites (Fig. 3) showed diffraction peaks (2θ) at 7.4° and 5.7°, respectively. The basal spacing of MMT was 1.18 nm, while it was 1.54 nm for PA–MMT composite. The peak shifting from higher diffraction angle to lower diffraction angle, and increment in the basal spacing of PA–MMT composite compared to MMT clearly supported the

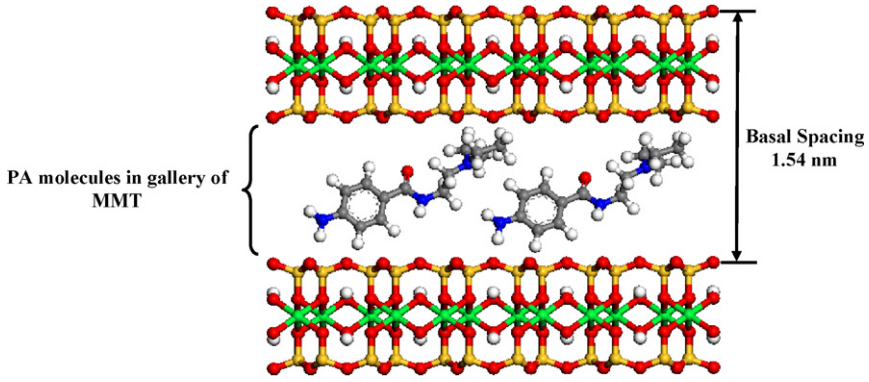

Schematic 1. Probable structural arrangement of PA into interlayer gallery of MMT.

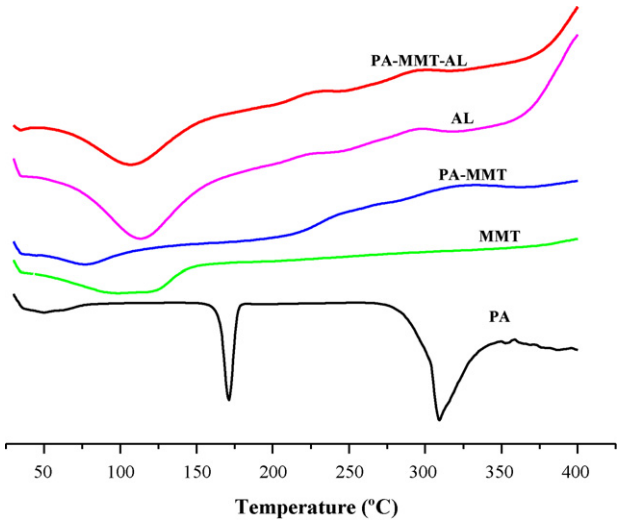

Fig. 6. DSC analysis of PA, MMT, PA–MMT, AL and PA–MMT–AL.

intercalation of PA into the interlayer of MMT. PA conformation is conceptually illustrated in Fig. 4 (Accelreys MS Modelling 3.2). The vertical dimension of the PA molecule is ~0.49 nm. Considering a silicate layer thickness of 0.96 nm, PA expanded the interlayer space by 0.58 nm, corresponds to a vertical orientation of the PA cations in a monolayer of MMT (Schematic 1).

FT-IR spectrum of PA, MMT, PA–MMT and PA–MMT–AL are shown in Fig. 5. AL showed asymmetric and symmetric stretching vibrations at 1616 and 1431 cm^{-1} due to carboxyl anions, and 1033 cm^{-1} for cyclic ether bridge for oxygen stretching. MMT showed band at 3443 cm^{-1} due to –OH stretching for interlayer water. The bands at 3624 and 3697 cm^{-1} are due to Al–OH and Si–OH. The shoulders and broadness of the structural –OH band are mainly due to contributions of several structural –OH groups occurring in the clay (Joshi et al., 2009a,b). The overlaid absorption peak at 1641 cm^{-1} attributed to –OH bending mode of adsorbed water, peak at 1032 cm^{-1} due to Si–O stretching (out-of-plane) and Si–O stretching (in-plane) vibration for layered silicates, respectively. Peaks at 914 and 775 cm^{-1} were attributed to Al–Al–OH and Al–Fe–OH, bending vibrations, respectively (Patel et al., 2007b). The peaks at 3216 and 3402 cm^{-1} are due to the primary amine and 1509 cm^{-1} for secondary amide bending of PA. The peak at 3318 and 3039 cm^{-1} were due to C–H stretching and peaks at 1394 cm^{-1} attributed to C–H bending vibrations of PA.

Incorporation of MMT into AL caused a shift to a higher wave number and the intensity of COO^- stretching peaks of AL decreases (Thaned and Satit, 2007). Thaned and Satit (2007) explained the change in the wave number of COO^- while AL interacts with MMT. The negative charge of the carboxyl groups may have an electrostatic interaction with the positively charged sites at the edges of MMT. The –OH stretching peak of the silanol group (SiOH) at 3697 cm^{-1} disappeared in the spectra of PA–MMT–AL composites, and the OH stretching peak of AL shifted to a higher wave number, which is an evidence of the intermolecular hydrogen bonding and

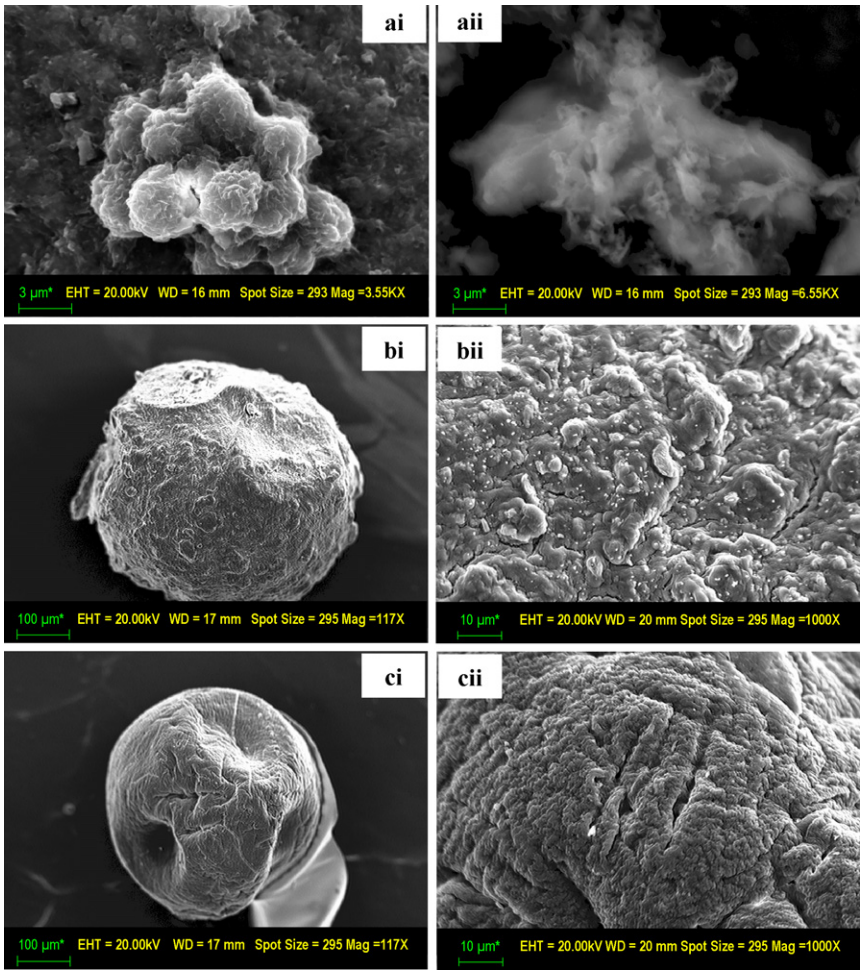

Fig. 7. SEM images of (ai) Pristine MMT (bi); PA–MMT–AL nanocomposite bead; (ci) PA–MMT–AL–CS nanocomposite bead; (aii) PA–MMT hybrid; (bii) surface images of PA–MMT–AL nanocomposite bead; and (cii) PA–MMT–AL–CS nanocomposite bead.

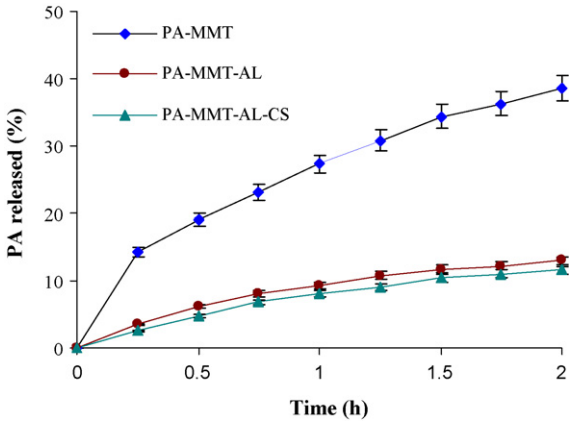

Fig. 8. Release profiles of PA in gastric fluid (pH 1.2) at 37 ± 0.5 °C.

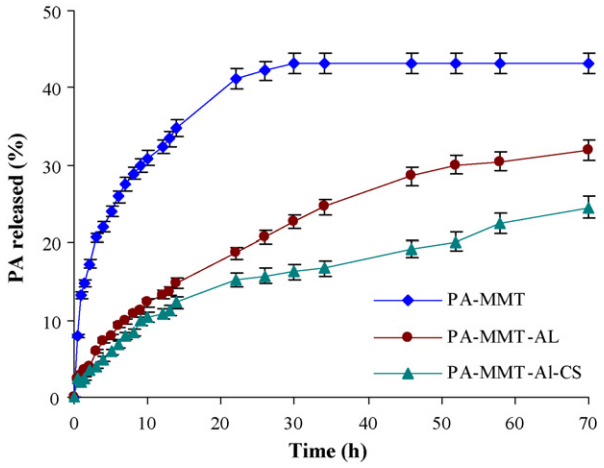

Fig. 9. Release profiles of PA in intestinal fluid (pH 7.4) at 37 ± 0.5 °C.

electrostatic forces between AL and MMT as confirmed by FT-IR studies.

3.2.2. Thermal stability of PA in MMT galleries

Thermal stability of PA in MMT galleries were analyzed by DSC of the PA, MMT, AL, PA–MMT and PA–MMT–AL (Fig. 6). DSC curves of pristine MMT gave a peak at 120 °C due to loss of water, whereas the powder of AL gave broad endothermic peak at 121 °C due to its thermal decomposition. The PA showed a sharp endothermic peak at 171 °C, corresponds to its melting temperature and second sharp endothermic peaks at 310 °C due to its degradation. However, these peaks were not observed in the DSC curves of PA–MMT composites. The PA–MMT–AL nanocomposites showed broad peak having similar pattern as that of AL, indicating the PA–MMT composites were uniformly dispersed in AL matrices at molecular level.

3.2.3. Morphology observation of the beads

Morphological study of PA–MMT/AL/CS composites beads is shown in Fig. 7. Fig. 7ai indicates nearly spherical MMT clusters, approximately 1 μm in diameter. The PA loaded MMT showed a disperse form (Fig. 7aii). In contrast, PA–MMT dispersion entrapped within AL beads depicts the spherical and rough nature of the bead Fig. 7(bi, bii). PA–MMT–AL–CS beads Fig. 7(ci, cii) showed extended smooth spherical shape due to the coating of CS on the surface of the PA–MMT–AL beads.

3.3. In vitro drug release study

The PA release profiles from the composites were observed both in gastric (pH 1.2) and intestinal environments (pH 7.4). Approximately 38% of the intercalated PA was released within 2 h from PA–MMT composite (Fig. 8). While in the case of formulations modified using AL and CS significantly reduced the PA release in the gastric environment. ~13 and 11% of PA was released from PA–MMT–AL and PA–MMT–AL–CS composites beads in 2 h. The negligible PA release from AL and CS coated composites as compared to PA–MMT composite in the gastric fluids was due to the fact that in acidic medium AL rapidly changed to water-insoluble alginic acid, consequently did not allowed PA to release in the media (Shilpa et al., 2003; Dai et al., 2008; Pongjanyakul, 2009).

In the phosphate buffer, release of PA from PA–MMT composite was ~17% in 2 h, ~30% in the first 10 h and 43% within 30 h, and remained constant up to 70 h (Fig. 9). While, in the case of PA–MMT–AL, and PA–MMTAL–CS composites beads, 4 and 3.5% in 2 h and 13 and 11% in 10 h PA was released. The maximum amount of PA released was found to be 32 and 25%, respectively up to 70 h. These results indicated that the release rate is faster in PA–MMT composite as compared to PA–MMT–AL/CS composites beads. Controlled release of PA was observed in the case of PA–MMT–AL/CS composites due to synergic effect of AL and MMT. The plateau for the release pattern of PA reached more rapidly in the case of PA–MMT composite as compared to the PA–MMT–AL/CS composites. The degree of swelling and disintegration of AL increased in the intestinal fluids, resulted in slow and controlled release behavior of PA from PA–MMT–AL composites. Moreover, CS was able to retard the PA release from PA–MMT–AL–CS composite. Therefore, compounding of PA–MMT composite with AL and further coating with CS seems to have a desirable effect to achieve site-specific delivery of PA.

3.4. Drug release kinetics

The values of correlation coefficient (r^2) and rate constants (k) for Higuchi and Korsmeyer–Peppas kinetic models are shown in Table 2. Taking into account the value of n, PA release from PA–MMT composite followed the diffusion controlled mechanism (fickian diffusion), while PA–MMT–AL/CS nanocomposites followed anomalous (non-fickian) diffusion.

Table 2
Expected parameters and drug release kinetic models for various formulations.

Kinetic models	Parameters	Formulations PA–MMT		PA–MMT–AL (1:1.4%, w/w)		PA–MMT–AL–CS (1:1.4%, w/w)	
		pH 1.2	pH 7.4	pH 1.2	pH 7.4	pH 1.2	pH 7.4
Higuchi	r^2	0.9938	0.9920	0.9933	0.9882	0.9928	0.9954
	k_H	26.598	8.6288	9.8584	4.240	10.053	3.879
Korsmeyer–Peppas	r^2	0.9874	0.9960	0.9947	0.9909	0.9856	0.9924
	n	0.4631	0.3917	0.5568	0.6533	0.7211	0.7221
	K_{KP}	0.7171	0.2985	0.7059	0.0866	0.6582	0.0776

4. Conclusion

The intercalations of PA into the interlayer of MMT via ion exchange mechanism have been achieved. The prepared PA–MMT composite was successfully compounded within AL and further coated with CS. The release performance of PA was found to be retarded in PA–MMT–AL/CS composite in the gastric environment compare to PA–MMT composite. Site-specific delivery of PA was effectively achieved using AL and CS. Release of PA from PA–MMT composite followed the diffusion controlled mechanism (fickian diffusion), while from PA–MMT–AL/CS composites followed Anomalous (non-fickian) diffusion based on kinetic models.

Acknowledgments

We are thankful to Council of Scientific and Industrial Research (CSIR) for funding under Network Project: NWP 0010; to Dr. P. Bhatt (XRD), Mr. V. Agarwal (FT-IR), Mrs. Sheetal patel (DSC) and Mr. Chandrakant (SEM) of the analytical section of the institute. The authors are thankful to Mr. G.P. Dangi for the design of computational model.

References

An, J., Geib, S.J., Rosi, N.L., 2009. Cation-triggered drug release from a porous zinc-adeninate metal-organic framework. J. Am. Chem. Soc. 131, 8376–8377.

Bergaya, F., Theng, B.K.G., Lagaly, G., 2006. Handbook of Clay Science, 1st edition. Elsevier Publication, Amsterdam.

Dai, Y.N., Li, P., Zhang, J.P., Wang, A.Q., Wei, Q., 2008. A novel pH sensitive N-succinyl chitosan/alginate hydrogel bead for nifedipine delivery. Biopharm. Drug Dispos. 29, 173–184.

Danielly, J., De Jong, R., Radke-Mitchell, L.C., Uprichard, A.C.G., 1994. Procainamide-associated blood dyscrasias. Am. J. Cardiol. 74, 1179–1180.

Depan, D., Kumar, A.P., Singh, R.P., 2009. Cell proliferation and controlled drug release studies of monohybrids based on chitosan-g-lactic acid and montmorillonite. Acta Biomater. 5, 93–100.

Denkbas, E.B., Ottenbrite, R.M., 2006. Perspectives on chitosan drug delivery systems based on their geometries. J. Bio. Comp. Polym. 21, 351–368.

Dong, Y., Feng, S.S., 2005. Poly(D,L-lactide-co-lycolide)/montmorillonite nanoparticles for oral delivery of anticancer drugs. Biomaterials 26, 6068–6076.

Ellenbogen, K.A., Wood, M.A., Gilligan, D.M., 1998. Intravenous procainamide. Cardiol. Elect. Rev. 2, 179–181.

Gerstl, Z., Nasser, A., Mingelgrin, U., 1998. Controlled release of pesticides into water from clay–polymer formulations. J. Agric. Food Chem. 46, 3803–3809.

Joshi, G.V., Kevadiya, B.D., Patel, H.A., Bajaj, H.C., Jasra, R.V., 2009a. Montmorillonite as a drug delivery system: intercalation and in vitro release of Timolol maleate. Int. J. Pharm. 374, 53–57.

Joshi, G.V., Patel, H.A., Kevadiya, B.D., Bajaj, H.C., 2009b. Montmorillonite intercalated with vitamin B_1 as drug carrier. Appl. Clay Sci. 45, 248–253.

Joshi, G.V., Patel, H.A., Bajaj, H.C., Jasra, R.V., 2009c. Intercalation and controlled release of vitamin B6 from montmorillonite–vitamin B6 hybrid. Colloid Polym. Sci. 287, 1071–1076.

Kevadiya, B.D., Joshi, G.V., Patel, H.A., Ingole, P.G., Mody, H.M., Bajaj, H.C., 2009. Montmorillonite–alginate nanocomposites as a drug delivery system: intercalation and in vitro release of vitamin B_1 and vitamin B_6. J. Biomater. Appl., doi:10.1177/0885328208344003.

Korsmeyer, R.W., Gurny, R., Doelker, E., Buri, P., Peppas, N.A., 1983. Mechanisms of solute release from porous hydrophilic polymers. Int. J. Pharm. 15,25–35.

Lee, B.H., Subramanian, S.Y., Lin, X., Nelson, W.G., 2005. Procainamide is a specific inhibitor of DNA methyltransferase-I. J. Biol. Chem. 280, 40749–40756.

Lin, F.H., Lee, Y.H., Jian, C.H., Wong, J.M., Shieh, M.J., Wang, C.Y., 2002. A study of purified montmorillonite intercalated with 5-fluorouracil as drug carrier. Biomaterials 23, 1981–1987.

Lin, F.H., Chen, C.H., Winston, T.K., Kuo, C.T., 2006. Modified montmorillonite as vector for gene delivery. Biomaterials 27, 3333–3338.

Manuel Fernandez-Perez, M., Villafranca-Sanchez, E., González-Pradas, F., Martinez-Lopez, Flores-Cespedes, F., 2000. Controlled release of carbofuran from an alginate–bentonite formulation: water release kinetics and soil mobility. J. Agric. Food Chem. 48, 938–943.

Markland, P., Amidon, G.L., Yang, V.C., 1999. Modified polypeptides containing gama-benzyl glutamic acid as drug delivery platforms. Int. J. Pharm. 178, 183–192.

Mohanambe, L., Vasudevan, S., 2005. Anionic clays containing anti-inflammatory drug molecules: comparison of molecular dynamics simulation and measurements. J. Phys. Chem. B 109, 15651–15658.

Park, J.K., Choy, Y.B., Oh, J.M., Kim, J.Y., Hwang, S.J., Choy, 2008. Controlled release of donepezil intercalated in smectite clays. Int. J. Pharm. 359, 198–204.

Pasparakis, G., Bouropoulos, N., 2006. Swelling studies and in vitro release of verapamil from calcium alginate and calcium alginate–chitosan beads. Int. J. Pharm. 323, 34–42.

Patel, H.A., Somani, R.S., Bajaj, H.C., Jasra, R.V., 2006. Nanoclays for polymer nanocomposites, paints, inks, greases and cosmetics formulations, drug delivery vehicle and waste water treatment. Bull. Mater. Sci. 29, 133–145.

Patel, H.A., Somani, R.S., Bajaj, H.C., Jasra, R.V., 2007a. Synthesis and characterization of organic bentonite using Gujarat and Rajasthan clays. Curr. Sci. 92, 1004–1009.

Patel, H.A., Somani, R.S., Bajaj, H.C., Jasra, R.V., 2007b. Preparation and characterization of phosphonium montmorillonite with enhanced thermal stability. Appl. Clay Sci. 35, 194–200.

Pongjanyakul, T., 2009. Alginate–magnesium aluminum silicate films: importance of alginate blocks structures. Int. J. Pharm. 365, 100–108.

Shilpa, A., Agrawal, S.S., Ray, A.R., 2003. Controlled delivery of drugs from alginate matrix. J. Macromol. Sci. C Polym. Rev. C 43, 187–221.

Sintov, A., Levy, R.J., 1997. Polymeric drug delivery of enzymatically degradable pendant agents: peptidyl-linked procainamide model system studies. Int. J. Pharm. 146, 55–62.

Sun, B., Ranganathan, B., Feng, S.S., 2008. Multifunctional poly(D,L-lactide-co-glycolide)/montmorillonite (PLGA/MMT) nanoparticles decorated by Trastuzumab for targeted chemotherapy of breast cancer. Biomaterials 29, 475–486.

Thaned, P., Satit, P., 2007. Sodium AL-magnesium aluminum silicate composite gels: characterization of flow behavior, micro-viscosity, and drug diffusivity. AAPS Pharm. Sci. Technol. 8, E1–E7.

Tonnesen, H.H., Karlsen, J., 2002. Alginate in drug delivery systems. Drug Dev. Ind. Pharm. 28, 621–630.

Wang, X., Du, Y., Lueo, J., 2008. Biopolymer/montmorillonite nanocomposite: preparation, drug-controlled release property and cytotoxicity. Nanotechnology, doi:10.1088/0957-4484/19/6/065707.

Zheng, J.P., Luan, L., Wang, H.Y., Xi, L.F., Yao, K.D., 2007. Study on ibuprofen/montmorillonite intercalation composites as drug release system. Appl. Clay Sci. 36, 297–301.